


Expression of human HIPKs in *Drosophila* demonstrates their shared and unique functions in a developmental model

Stephen D. Kinsey , Justin P. Vinluan, Gerald A. Shipman, and Esther M. Verheyen *

Department of Molecular Biology and Biochemistry, Centre for Cell Biology, Development and Disease, Simon Fraser University, Burnaby, BC V5A 1S6, Canada

*Corresponding author: Email: everheye@sfu.ca

Abstract

Homeodomain-interacting protein kinases (HIPKs) are a family of four conserved proteins essential for vertebrate development, as demonstrated by defects in the eye, brain, and skeleton that culminate in embryonic lethality when multiple HIPKs are lost in mice. While HIPKs are essential for development, functional redundancy between the four vertebrate HIPK paralogues has made it difficult to compare their respective functions. Because understanding the unique and shared functions of these essential proteins could directly benefit the fields of biology and medicine, we addressed the gap in knowledge of the four vertebrate HIPK paralogues by studying them in the fruit fly *Drosophila melanogaster*, where reduced genetic redundancy simplifies our functional assessment. The single *hipk* present in the fly allowed us to perform rescue experiments with human *HIPK* genes that provide new insight into their individual functions not easily assessed in vertebrate models. Furthermore, the abundance of genetic tools and established methods for monitoring specific developmental pathways and gross morphological changes in the fly allowed for functional comparisons in endogenous contexts. We first performed rescue experiments to demonstrate the extent to which each of the human HIPKs can functionally replace *Drosophila* *Hipk* for survival and morphological development. We then showed the ability of each human HIPK to modulate Armadillo/ β -catenin levels, JAK/STAT activity, proliferation, growth, and death, each of which have previously been described for *Hipks*, but never all together in comparable tissue contexts. Finally, we characterized novel developmental phenotypes induced by human HIPKs to gain insight to their unique functions. Together, these experiments provide the first direct comparison of all four vertebrate HIPKs to determine their roles in a developmental context.

Keywords: HIPK2; *Drosophila*; HIPK1; HIPK3; HIPK4; development; imaginal discs; genetic rescue

Introduction

Homeodomain-interacting protein kinases (HIPKs) are a family of conserved serine/threonine kinases that are necessary for development in both invertebrate and vertebrate organisms (Blaquiere and Verheyen 2017). In *Drosophila melanogaster*, combined maternal and zygotic loss of the single homolog *hipk* (referred to hereafter as *dhipk*) results in early embryonic lethality, while zygotic loss alone results in pupal lethality (Lee et al. 2009a). Experiments performed in mice, which like other vertebrates have four *Hipk* genes (*Hipks1-4*), have demonstrated that knockouts of individual genes are viable, while homozygous loss of both *Hipk1* and *Hipk2* results in embryonic lethality. The viability of single *Hipk* knockouts in vertebrates has been attributed to functional redundancy between the paralogues, where the activity of the remaining HIPKs compensates for the loss (Isono et al. 2006). Interestingly, *Hipk1/2* double knockout mice share phenotypes with *dhipk* mutant flies, such as defects in the eye, head, and overall patterning (Isono et al. 2006; Lee et al. 2009a; Inoue et al. 2010).

The research showing functional redundancy between HIPK1 and HIPK2 provides evidence for their similar developmental roles. It is therefore surprising that comparable studies have not been performed with the other family members. The kinase

domain is the region of greatest similarity between vertebrate HIPK paralogues, a similarity that extends to the orthologous *dHipk* (Figure 1A). In addition, HIPK1, HIPK2, HIPK3, and *dHipk* share other structural features outside of the kinase domain that have been implicated in protein-protein interactions and in regulating *Hipk* stability and localization (Rinaldo et al. 2008; Blaquiere and Verheyen 2017). Despite the similarity of *Hipk* proteins, mutant mice demonstrate distinct phenotypes. For example, *Hipk1* knockout mice appear grossly normal, *Hipk2* knockout mice exhibit impaired adipose tissue development, smaller body size, and higher incidence of premature death, *Hipk3* knockout mice exhibit impaired glucose tolerance, and male *Hipk4* knockout mice are infertile due to abnormal spermiogenesis (Kondo et al. 2003; Chalazonitis et al. 2011; Shojima et al. 2012; Sjölund et al. 2014; Crapster et al. 2020). Unfortunately, these reported phenotypes come from a small number of articles focusing primarily on different tissues, so it is unclear if these variable phenotypes are the result of different spatial temporal expression patterns, different protein functions, or a combination of the two. RNA sequencing projects have demonstrated that human HIPK1, HIPK2, and HIPK3 are broadly expressed throughout the adult body and that HIPK4 is restricted to the brain and testes, however the

Received: August 12, 2021. Accepted: September 21, 2021

© The Author(s) 2021. Published by Oxford University Press on behalf of Genetics Society of America.

This is an Open Access article distributed under the terms of the Creative Commons Attribution License (<https://creativecommons.org/licenses/by/4.0/>), which permits unrestricted reuse, distribution, and reproduction in any medium, provided the original work is properly cited.

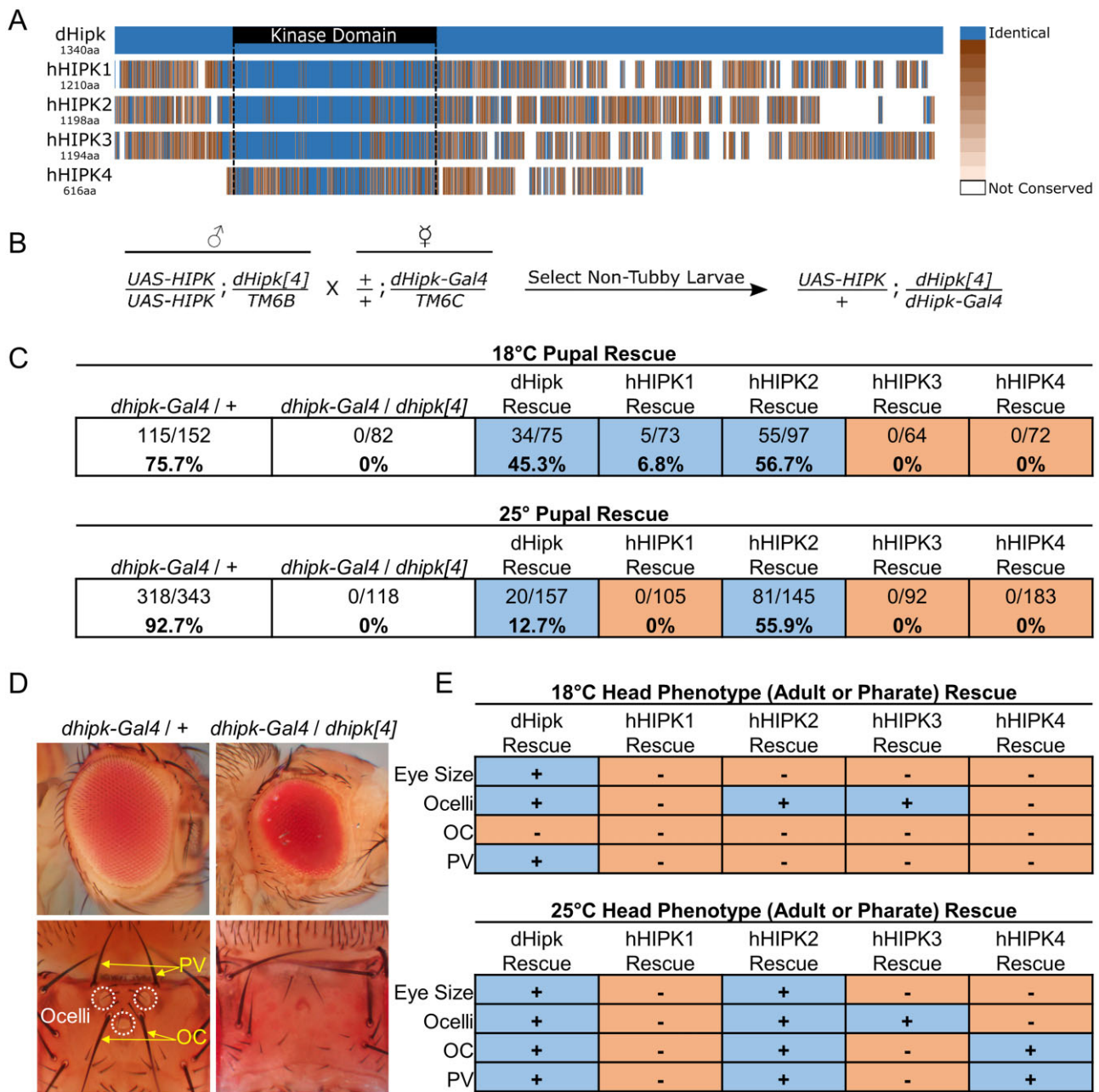


Figure 1 Human HIPKs rescue *dhipk* mutant phenotypes. (A) The amino acid sequence of the four human HIPKs are aligned to dHipk using the NCBI constraint-based multiple alignment tool (COBALT) (Papadopoulos and Agarwala 2007). Dark blue indicates the amino acid at a given position is identical to dHipk at the aligned position, while shades of orange indicate a range between high similarity (dark orange) and low similarity (light orange), and white indicates lack of conservation between the human HIPK and dHipk. (B) The cross scheme used to generate *dhipk* mutant flies that expressed UAS-hHIPKs in the *dhipk* expression domain. A male fly homozygous for a UAS-hHIPK transgene on the 2nd chromosome and heterozygous for the *dhipk*[4] mutant on the 3rd chromosome over the balancer *TM6B* was crossed to a female fly with a wild-type 2nd chromosome and heterozygous for *dhipk-Gal4* on the 3rd chromosome over the balancer *TM6C*. Both the *TM6C* and *TM6B* balancer chromosomes produce a tubby phenotype, therefore nontubby progeny pupae were scored for each cross. (C) Tables state the number of flies that successfully eclosed from pupal cases at both 18°C and 25°C. White shading indicates the control crosses. Experimental crosses are shown with blue or orange shading to indicate successful or failed eclosion/survival, respectively, with both the ratio and the percent of flies rescued listed. (D) Representative eyes (top) and dorsal head structures (bottom) from heterozygous *dhipk-Gal4*/+ flies and transheterozygous *dhipk-Gal4*/*dhipk*[4] flies, highlighting the reduced eye size, and loss of ocelli, posterior vertical bristles (PV), and ocellar bristles (OC) in *dhipk* mutants. (E) Tables show which Hipks significantly rescue the *dhipk* mutant head phenotypes when expressed in the *dhipk-Gal4*/*dhipk*[4] mutant background at both 18°C and 25°C, based on graphs and statistical analysis described in Supplementary Figure 2.

patterns of HIPK1-4 expression during development is unclear (Uhlén et al. 2015).

The difficulty of uncovering the extent of functional redundancy for vertebrate HIPKs has led to much of the work on these

proteins being done in cell culture using exogenously expressed proteins to assess localization, pathway alterations, protein-protein interactions, and altered kinetic activities. While useful for some assays, the cell culture model is unsuitable for comparing

developmental functions due to inherent abnormalities in immortalized cell lines, and lack of cellular diversity. One study directly compared all vertebrate HIPKs using cell culture, though its analysis was focused on kinetic activity and cellular localization rather than developmental potential (Van der Laden et al. 2015). Despite the lack of direct comparison between vertebrate HIPKs, striking similarities have been observed for the functions of *Drosophila* dHipk and some vertebrate HIPKs, primarily HIPK2, in modulating developmental signaling pathways, including WNT, JNK, Hippo, and JAK/STAT (Rochat-Steiner et al. 2000; Hofmann et al. 2003, 2005; Lan et al. 2007; Lee et al. 2009b; Louie et al. 2009; Hikasa and Sokol 2011; Huang et al. 2011; Swarup and Verheyen 2011; Chen and Verheyen 2012; Poon et al. 2012; Shimizu et al. 2014).

Recent studies have successfully used the fly as a model to study the functions of human proteins, especially in cases where they fly had reduced redundancy for the candidate gene (McGurk et al. 2015; Ugur et al. 2016; Link and Bellen 2020; Baldridge et al. 2021). We therefore saw the fly as a useful model to compare the functional equivalency of the four wild-type vertebrate HIPKs. The single *Drosophila* dHipk and the abundance of tools available to study developmental signaling in *Drosophila* tissues allow for easy assessment of pathway alterations caused by vertebrate HIPKs. Therefore, we used the fly to determine if the four human HIPKs were capable of performing the same functions in a developmental model. By expressing hHIPKs in both a *dhipk* knockout background, and in multiple tissues of a wild-type genetic background, our comparisons of HIPKs in the fly identified functional similarities between hHIPKs in overall development, as well as unique differences when assessing their activity in identical developing epithelial tissues.

Materials and methods

Fly stocks and genetic crosses

Previously described fly strains used in this work are **1:** *w¹¹¹⁸*, **2:** *dhipk-Gal4* (*hipk*[BG00855], BDSC #12779), **3:** *UAS-GFP* (BDSC #5431), **4:** *UAS-pc^{RNAi}* (BDSC #33964), **5:** *UAS-e(z)^{RNAi}* (BDSC #36068), **6:** *UAS-sce^{RNAi}* (BDSC #67924), **7:** *UAS-ph-d^{RNAi}* (BDSC #63018) **8:** *dhipk⁴* (Lee et al. 2009a), **9:** *dpp-Gal4/TM6B* (Staehling-Hampton et al. 1994), **10:** *UAS-HA-dhipk^{attp40}* (Tettweiler et al. 2019), **11:** *eyFLP; act>y⁺>Gal4, UAS-GFP* (Pagliarini and Xu 2003). The details of how *UAS-myc-hHIPK1^{attp40}*, *UAS-myc-hHIPK2^{attp40}*, *UAS-myc-hHIPK3^{attp40}*, and *UAS-myc-hHIPK4^{attp40}* were generated for this work is detailed in the section titled “Generation of plasmids and transgenic *UAS-hHIPK* fly stocks.” *dhipk* mutant rescue experiments were performed at 18°C and 25°C to determine the ideal *Hipk* expression levels by modulating the expression of Gal4-driven *UAS-Hipk* constructs, while experiments using *dpp-Gal4* were performed at 29°C to increase *UAS-Hipk* expression. Flies were raised on standard media composed of 0.8 g agar, 2.3 g yeast, 5.7 g cornmeal, and 5.2 mL molasses per 100 mL. “BDSC” is an acronym for the Bloomington *Drosophila* Stock Center.

Terminology

As this study investigates human proteins expressed in *Drosophila*, we wanted to clearly indicate which species of protein is specified in each experiment. Throughout this paper, *D. melanogaster* *Hipk* protein is written “dHipk” while mutants or DNA are referred to as *dhipk*, human HIPKs are written as “hHIPKs,” and in cases where reference is made to proteins from both species, “Hipks” is used.

Generation of plasmids and transgenic *UAS-hHIPK* fly stocks

Plasmids containing the cDNA for human HIPKs were generously provided by two groups. Dr. Lienhard Schmitz gifted a plasmid containing *hHIPK1* isoform 1, and Dr. Seong-Tae Kim provided us plasmids containing *hHIPK3* isoform 2 and *hHIPK4*. The cDNA for *hHIPK2* isoform 1 was synthesized by GenScript® to match the NCBI reference sequence NM_022740.4. In cases where the gifted cDNAs did not exactly correspond to the translated NCBI reference protein sequences (NP_938009.1 for *hHIPK1*, NP_001041665.1 for *hHIPK3*, and NP_653286.2 for *hHIPK4*), we performed site-directed mutagenesis using the GeneArt™ Site-Directed Mutagenesis PLUS system to correct the cDNA sequence. The cDNAs that corresponded to these reference sequences were then tagged with N-terminal Myc-epitope tags before being cloned into a pUAST-attB backbone vector using NotI and XhoI restriction sites for *hHIPK1* and *hHIPK2*, BglII and KpnI sites for *hHIPK3*, and BglII and XhoI sites for *hHIPK4*. The four pUAST-attB-Myc-hHIPK plasmids were then sent to BestGene Inc. for injection into *Drosophila* embryos containing an attP40 site, allowing for stable integration to identical sites on the second chromosome. The resulting fly stocks each contain a single Myc-hHIPK cDNA under the control of a UAS promoter that is expressed in any cell expressing a Gal4 transcription factor.

Adult *Drosophila* imaging and scoring rescue phenotypes

The pharate pupae and viable adults from the *dhipk* mutant viability rescue experiment were collected, and if necessary, gently removed from their pupal cases with dissecting tweezers before being immediately placed in 70% ethanol and stored at –20°C for preservation until they were photographed for the assessment and quantification of head phenotypes. Six randomly selected female flies from each cross were used for phenotype quantification. To image these flies, we used an 8-well BD Falcon CultureSlide (REF 354118) modified to have each well filled 1/3 with SYLGARD™ 184 (Supplementary Figure S5). Insect pins were bent at 90° and pinned into the solidified SYLGARD so that the 90° bend was located near the top of the plastic well. Immediately before imaging, flies were removed from 70% ethanol at –20°C to individual wells filled with 70% ethanol at room temperature and pinned to the planted insect pins while remaining submerged. The slides were then topped off with excess 70% ethanol before a coverslip was placed atop the wells. A resulting slide contained six female flies of the same genotype pinned at a stable position for imaging near the surface of the coverslip, while remaining submerged in ethanol. The ethanol was required to prevent flies drying out during imaging, and the coverslip was required to prevent vibrations on the surface of the ethanol that interfered with imaging. The same six flies were photographed three times to capture each eye (two images per fly) and the top of the head (one image per fly). Lighting was provided by an LED strip modified to encircle the CultureSlide, and a folded white tissue was placed under the CultureSlide to obtain a white/grey background.

Adult wings and legs were dissected in ethanol, then gently dried on a paper towel before being submerged in a small drop of Aquatex® (Sigma-Aldrich #1.08562) and covered in a coverslip. Small weights (EM stubs) were then placed on the coverslips while being heated to 60°C for 1 h. All adult phenotypes were imaged using a Zeiss Axioplan2 microscope with an Optika C-P6 camera system.

To determine pupal lethality in the *dhipk* mutant rescue experiment, crosses were performed with 24-h egg lays, and all non-Tubby pupal cases were scored as eclosed or pharate 5 days after flies were expected to have eclosed.

HIPK protein sequence alignment

After confirming that our cDNA sequences correctly translated to the NCBI reference protein sequences for hHIPK1 isoform 1 (NP_938009.1), hHIPK2 isoform 1 (NP_073577.3), hHIPK3 isoform 2 (NP_001041665.1), hHIPK4 (NP_653286.2), and dHipk isoform A (NP_612038.2), each of the hHIPK sequences were individually compared to dHipk using the NCBI COBALT tool (Papadopoulou and Agarwala 2007). dHipk was set as the anchor. The FASTA alignment for this comparison was then downloaded and opened in Jalview (version 2.11.1.2) to extract the numerical conservation data between each of the hHIPKs and dHipk individually (Waterhouse et al. 2009). The numerical conservation data (from 0=no conservation, to 11=identical amino acid) was then extracted and sent to Microsoft Excel (Excel 365), where numerical columns were converted to a color gradient. An image of the alignment was then exported as a PNG to Inkscape (version 0.92.4) for annotation, based on the NCBI annotation of the kinase domain.

Immunocytochemistry and microscopy

Late third instar larval imaginal discs were dissected and stained using previously described methods (Blaquiere et al. 2018). The following primary antibodies were used: mouse anti-Ubx (1:50, DSHB Ubx FP3.38) mouse anti-Scr (1:50, DSHB anti-Scr 6H4.1), mouse anti-Arm (1:10 DSHB N27A1 Armadillo), mouse anti-Wg (1:50, DSHB 4D4), rabbit anti-PH3 Ser10 (1:500, Cell Signaling #9701S). Imaginal discs were imaged on a Zeiss LSM 880. Images were processed in FIJI.

Clonal analysis

FLP-out clones expressing UAS-Hipks positively marked with RFP were generated by exposing 1st instar larvae of the genotype *hsflp¹¹²/+*; *10xStat92E-GFP/UAS-Hipk*; *actin>CD2>Gal4*, UAS-RFP/+ to a 37°C water bath for 12 min, followed by incubation at 29°C until larvae reached the wandering 3rd instar stage, as performed by Wong et al. (2019). Wing imaginal discs were then dissected, stained, and imaged as above.

PH3 and TUNEL assay quantification using wing imaginal discs

Dual PH3 and TUNEL assay staining was performed by first completing the normal wing disc dissection, fixing, washing, and primary antibody treatment protocol noted previously for PH3 (1:500 in block, Cell Signaling #9701S). Before secondary antibody staining, TUNEL staining was performed using the Roche *In Situ* Cell Death Detection Kit, TMR Red (Version 12, Cat. No. 12 156 792 910). Once the tissues were washed after the primary antibody treatment, the wash was removed, and 100 µl of combined TUNEL assay components (92.7 µl labeling solution + 8.3 µl enzyme solution) was added to the tissues in a 1.6 mL Eppendorf tube, along with 1:1000 goat α -rabbit fluorophore conjugated secondary antibody (Jackson ImmunoResearch, product # 711-605-152). The tissues were then incubated overnight (~16h) on a rocker in the dark at 4°C. Staining reagents were then removed, and samples were rinsed quickly with PBT before staining for 30 min with 1:500 DAPI solution. After DAPI staining, four more 10-minute washes were performed before wing discs were separated from other tissues and mounted in 70% glycerol on

microscope slides. Wing imaginal discs were imaged as described in the previous section. Using FIJI (Schindelin et al. 2012, 2015; Schneider et al. 2012), the area of the whole wing imaginal disc and *dpp-GFP* domains were measured, and PH3 or TUNEL positive cells were counted within each region automatically using the Analyze → Analyze Particles tool after thresholding. The change in concentration of PH3 or TUNEL positive cells between the *dpp-GFP* domain and the rest of the disc was then calculated.

RNA extraction and qPCR

RNA extractions were performed using the Qiagen RNeasy[®] Plus Mini Kit (#74134). RNA that was used to confirm reduced *dhipk* mRNA in *dhipk* mutant and rescue crosses, as well as verify the correct hHIPK expression in the rescue crosses, was collected from four combined wandering 3rd instar larvae (two male and two female) for each cross. Larvae were washed in PBS before being spot dried on a clean paper towel and transferred to 300 µl buffer RLT Plus, supplemented with freshly added β -mercaptoethanol to 1%. Larvae were homogenized with pestles by hand in 1.6 mL tubes before being centrifuged for 3 min at maximum speed to pellet debris. Supernatant was transferred to a gDNA Eliminator spin column, with the remaining RNA extraction steps following the manufacturer's instructions.

cDNA synthesis was performed using ABM[®] OneScript[®] Plus cDNA Synthesis Kit (#G236). For each sample, 100 ng mRNA was used in combination with Oligo (dT) primers to perform first-strand cDNA synthesis of poly-adenylated mRNA following manufacturer's instructions. Resulting cDNA was diluted 1:5 before being used for qPCR.

qPCR for each sample/primer mix was performed in triplicate with 10 µl samples (technical replicates), utilizing Bioline's sensiFAST SYBR Lo-ROX Kit (#BIO-94005) on an Applied Biosystems QuantStudio 3. One microliter of diluted cDNA was used per reaction. Primers targeting *rp49* were used as reference targets.

Primers

rp49 F: AGCATACAGGCCCAAGATCG
rp49 R: TGTTGTCGATACCCTTGGGC
dhipk F: GCACCACAACCTGCAACTACG
dhipk R: ACGTGATGATGGTGCGAACTC
hHIPK1 F: GACCAGTGCAGCACAACCAC
hHIPK1 R: GCCATGCTGGAAGGTGTAGG
hHIPK2 F: GTCCACCAACCTGACCATGA
hHIPK2 R: GGAGACTTCGGGATTGGCTA
hHIPK3 F: GACATCAGCATTCCAGCAGC
hHIPK3 R: GCTGTCTTCTGTGCCCAAAG
hHIPK4 F: GCCTGAGAACATCATGCTGG
hHIPK4 R: GCGACTGGATGTATGGCTCC

Results

hHIPK1 and hHIPK2 rescue *dhipk* mutant lethality

As a first step in characterizing hHIPK functions in *Drosophila*, we wanted to test whether expression of hHIPKs using the Gal4/UAS system could rescue phenotypes caused by loss of *dhipk*. To do this, we combined two *dhipk* mutant alleles, *dhipk[4]* and *dhipk-Gal4*, to generate a transheterozygous (heteroallelic) knockout of *dhipk* (Figure 1B). The *dhipk[4]* mutant has a deletion removing 9 out of the possible 10 exons (Lee et al. 2009a), while the *dhipk-Gal4* mutant generated by the *Drosophila* Gene Disruption Project (insertion #BG00855) contains a Gal4 coding sequence inserted upstream of *dhipk* that effectively prevents its expression when

combined with the *dhipk[4]* allele (Supplementary Figure S1, A–D) (Bellen et al. 2004, 2011). In subsequent sections, *dhipk[4]/dhipk-Gal4* mutant flies are simply referred to as “*dhipk* mutants.” These *dhipk* mutants are 100% lethal prior to pupal eclosion, with pharate pupae dissected from pupal cases showing reduced eye size, loss of ocelli, and missing ocellar bristles (Figure 1, C and D). This knockout approach has two main benefits. First, it disrupts endogenous *dhipk* expression while allowing expression of UAS-driven transgenes in the endogenous *dhipk* domain due to the insertion of Gal4 coding sequences in the *dhipk* locus (Supplementary Figure S1, C and D). Second, this approach reduces the effect of secondary mutations present on chromosomes carrying the individual *dhipk* mutant alleles that may contribute to lethality when made homozygous.

To confirm that the *dhipk-Gal4* allele was capable of driving UAS-transgene expression in the appropriate tissues and stages, we first expressed a wildtype UAS-*dhipk* cDNA construct in the *dhipk* mutant background (Figure 1C). We expected a phenotypic rescue if the *dhipk-Gal4* allele correctly drove UAS expression in the endogenous *dhipk* domains. We raised these crosses at both 18°C and 25°C to assay the effects of two levels of transgene expression, since the activity of Gal4 and therefore level of expression of UAS transgenes is enhanced at higher temperatures (Duffy 2002). This was essential to determining optimal conditions, since our previous work has shown that overexpression of dHipp in a wildtype background at 29°C causes numerous phenotypes, including tumorigenic effects (Blaquiere et al. 2018; Wong et al. 2019, 2020). As expected, the majority of control flies heterozygous for the *dhipk-Gal4/+* allele successfully eclosed from pupae (92.7% at 25°C and 75.7% at 18°C) and 0% of *dhipk* mutant flies eclosed at either temperature, with death occurring at or before the pupal stage (Figure 1C). In the UAS-*dhipk* rescue experiment, 12.7% of flies eclosed at 25°C, and 45.3% of flies eclosed at 18°C, indicating that the *dhipk-Gal4* allele drives UAS-*dhipk* in a spatial and temporal pattern sufficiently similar to endogenous *dhipk* expression.

We next tested the ability of the four UAS-hHIPK transgenes to rescue *dhipk* mutant lethality (Figure 1C). To maintain consistency of transgene expression, we utilized targeted integration to insert each human and fly HIPK cDNA into the genome on the second chromosome at the engineered attp40 landing site as described in the methods. We found that UAS-hHIPK1 rescued 6.8% of *dhipk* mutants at 18°C, while it was unable to rescue at 25°C. In contrast, UAS-hHIPK2 rescued the lethality of 56.7% of *dhipk* mutants at 18°C, and 55.9% at 25°C, which was more effective than the rescue by UAS-*dhipk*. Finally, neither UAS-hHIPK3 nor UAS-hHIPK4 rescued the lethality of *dhipk* mutants (Figure 1C).

hHIPKs variably rescue *dhipk* mutant patterning phenotypes

Only UAS-hHIPK1 and UAS-hHIPK2 were able to rescue *dhipk* mutant lethality, however it was possible that the other hHIPKs could rescue minor *dhipk* mutant patterning phenotypes in fully formed, yet inviable, pharate adults dissected from their pupal cases. *dhipk* mutant flies that develop to the pharate adult stage have reduced compound eye size, and are missing the three ‘simple eyes’ called ocelli on the top of their heads (Figure 1D) (Lee et al. 2009a; Blaquiere et al. 2014). Ocellar and posterior vertical bristles are also lost in *dhipk* mutant pharate adults. Combined, the eye, ocelli, and bristle phenotypes are the most obvious external changes on pharate *dhipk* mutant flies. Therefore, we asked if UAS-hHIPKs could rescue these phenotypes. As with the *dhipk* mutant lethality rescue experiments, we carried out these

crosses at both 18°C and 25°C to modulate the degree of Gal4-driven expression of the transgenes (Figure 1E, Supplementary Figure S2).

While the rescue of *dhipk* mutant lethality by UAS-*dhipk* and UAS-hHIPKs was more effective at 18°C than it was at 25°C, this was not true for the head phenotypes. UAS-*dhipk* was able to significantly rescue each *dhipk* mutant phenotype when raised at 25°C but failed to rescue the ocellar bristle loss at 18°C (Figure 1E, Supplementary Figure S2). For the human HIPKs, UAS-hHIPK1 was unable to rescue any head phenotype at either 18°C or 25°C, despite rescuing lethality at 18°C. UAS-hHIPK2 significantly rescued all phenotypes at 25°C, but only rescued the loss of ocelli at 18°C. Finally, while UAS-hHIPK3 and UAS-hHIPK4 were unable to rescue *dhipk* mutant lethality, UAS-hHIPK3 rescued the loss of ocelli at both temperatures, and UAS-hHIPK4 rescued the loss of ocellar bristles and posterior vertical bristles at 25°C only. In addition, UAS-hHIPK4 caused a significant reduction in eye size compared to the *dhipk* mutant phenotype alone at both temperatures (Supplementary Figure S2). Together, these rescue experiments show that only human HIPKs 1 and 2 are capable of rescuing *dhipk* mutant lethality, while each of the human HIPKs can rescue a subset of the *dhipk* mutant head phenotypes.

hHIPKs act on dHipp target pathways

Next, we were interested in comparing the ability of human HIPKs to modulate specific signaling pathways known to be affected by dHipp. Our group has previously shown that dHipp and vertebrate HIPK2 are able to increase the stability of the key Wnt/Wingless effector protein Armadillo/ β -Catenin by inhibiting its ubiquitin-mediated degradation (Lee et al. 2009b; Swarup and Verheyen 2011). Therefore, we assessed the ability of human HIPKs to stabilize endogenous Armadillo (Arm) in *Drosophila* by expressing HIPKs using *dpp-Gal4*, which drives transgene expression in a small stripe of cells along the anterior-posterior boundary of the developing wing imaginal disc (Figure 2A). Arm is expressed ubiquitously and is enhanced in two stripes flanking the dorsal-ventral boundary of the wing disc due to high levels of Wingless signaling (Peifer et al. 1994). We quantified pixel intensity to compare Arm levels in cells expressing transgenes and in flanking wild-type cells (Figure 2B). Consistent with our previous results with dHipp, we found that hHIPK2, hHIPK3, and hHIPK4 expression significantly increased the amount of Arm at the dorsal-ventral boundary of wing imaginal discs, while hHIPK1 was unable to do so (Figure 2C).

Our group has recently demonstrated that dHipp is required for JAK/STAT signaling during *Drosophila* development (Tettweiler et al. 2019). We therefore assessed the ability of the four human HIPKs to enhance JAK/STAT signaling in the hinge region of the wing imaginal disc where endogenous JAK/STAT signaling is most prominent (Figure 2D). We used the 10xSTAT92E-GFP reporter containing ten STAT92E binding sites driving expression of an EGFP cDNA to provide a readout of JAK/STAT pathway activity (Bach et al. 2007). We generated random UAS-transgene expressing clones using the flip-out technique as described in the methods. RFP expression marks clones in which UAS-transgenes are expressed. We found that each of the four hHIPKs and dHipp variably caused an increase in endogenous JAK/STAT activity in clones found in the hinge region of the wing imaginal disc (Figure 2E, arrows).

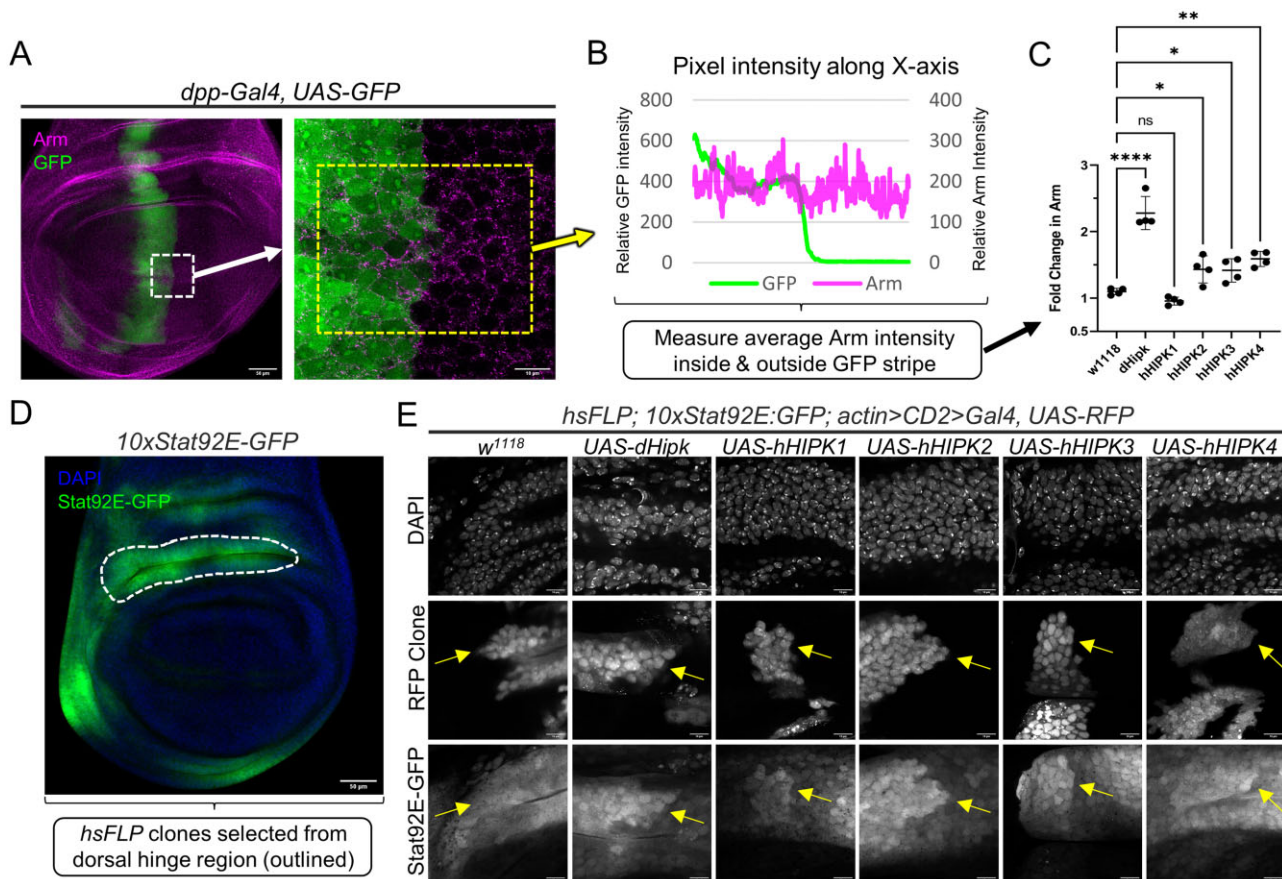


Figure 2 Human HIPKs phenocopy dHipk pathway alterations. (A) Representative image of a 3rd instar wing imaginal disc control sample expressing GFP in the *dpp-Gal4* domain, and counterstained for Armadillo (Arm). The left image is a zoomed-out version of the image on the right, meant to provide context to our region of interest, highlighted in the dashed white box. The image on the right is zoomed in to focus on the region where the *dpp-Gal4* domain (marked with GFP) intersects the dorsal-ventral boundary of the wing disc that contains stabilized Arm. (B) Four samples were imaged at this magnification per cross, and the pixel intensity across the x-axis of the region within the dashed yellow box (as shown in panel A) was measured using ImageJ and plotted. For each image, a graph was generated to define the region of GFP and transgene expression along the x-axis. Once defined, the average pixel intensity of Arm was measured across these regions. (C) The average pixel intensity of Arm in the indicated genotypes was measured using the method shown in panel B. To calculate the fold change in Arm, the Arm signal for the GFP positive region was divided by that of the GFP negative region. Error bars indicate the mean with a 95% confidence interval. A one-way ANOVA was performed followed by Dunnett's test to correct for multiple comparisons to *w1118* for each dataset. P-values for the statistical analyses performed correspond to the following symbols: ≥ 0.0332 (ns), < 0.0332 (*), < 0.0021 (**), < 0.0002 (***), < 0.0001 (****) (D) 3rd instar imaginal wing disc expressing the JAK/STAT pathway reporter 10xStat92E-GFP, co-stained for DNA (DAPI) in blue to highlight tissue morphology. The dorsal hinge region of the wing disc, surrounded in the dashed white line, was used in our assessment of HIPKs on JAK/STAT activity. (E) Flp-out clones of cells expressing UAS-Hipks were generated in the dorsal hinge region defined in Figure 2D. Clones were marked in RFP, with DAPI acting as a counterstain. Yellow arrows indicate RFP clone edges and the corresponding tissue areas showing 10xStat92E-GFP reporter expression. All images are from crosses performed at 29°C.

hHIPKs variably induce cell death and proliferation

Hipks have been shown to have variable and conflicting abilities to promote cell proliferation, tissue growth, and apoptosis through modulation of signaling pathways (Blaquiere and Verheyen 2017). Using a different *UAS-dHipk* insertion strain (*UAS-Hipk^{3M}*) which has higher expression levels than the *attP40* strain used in this work promotes cell proliferation and tissue growth in the wing imaginal disc (Blaquiere et al. 2018; Wong et al. 2019, 2020). Therefore, we tested the ability of dHipk and hHIPKs to promote cell proliferation, tissue growth, and apoptosis in those same assays.

Using *dpp-Gal4* to drive expression of *UAS-HIPKs* in combination with *UAS-GFP* to mark the expression domain, we imaged wing discs to detect the proliferation marker phosphorylated

histone 3 (PH3), and performed terminal deoxynucleotidyl transferase dUTP nick end labeling (TUNEL) to detect apoptosis (Figure 3, A–E) (Gavrieli et al. 1992). Comparing the concentration of PH3 and TUNEL in GFP positive and GFP negative tissues let us determine how each HIPK affected cell proliferation and apoptosis (Figure 3, B–D). Similarly, measuring the area of the GFP domain compared to the overall wing disc area allowed us to measure HIPK-mediated changes to tissue growth (Figure 3, B and E). Expression of dHipk or hHIPK3 caused a significant increase in PH3 in the wing disc, while no change was detected when hHIPK1, hHIPK2, or hHIPK4 were expressed (Figure 3C). Similarly, only dHipk and hHIPK3 caused a significant increase in the tissue size (Figure 3E). Finally, we found that dHipk and hHIPK1 significantly induce apoptosis in the wing imaginal disc, as we had seen with dHipk previously (Figure 3D) (Blaquiere et al.

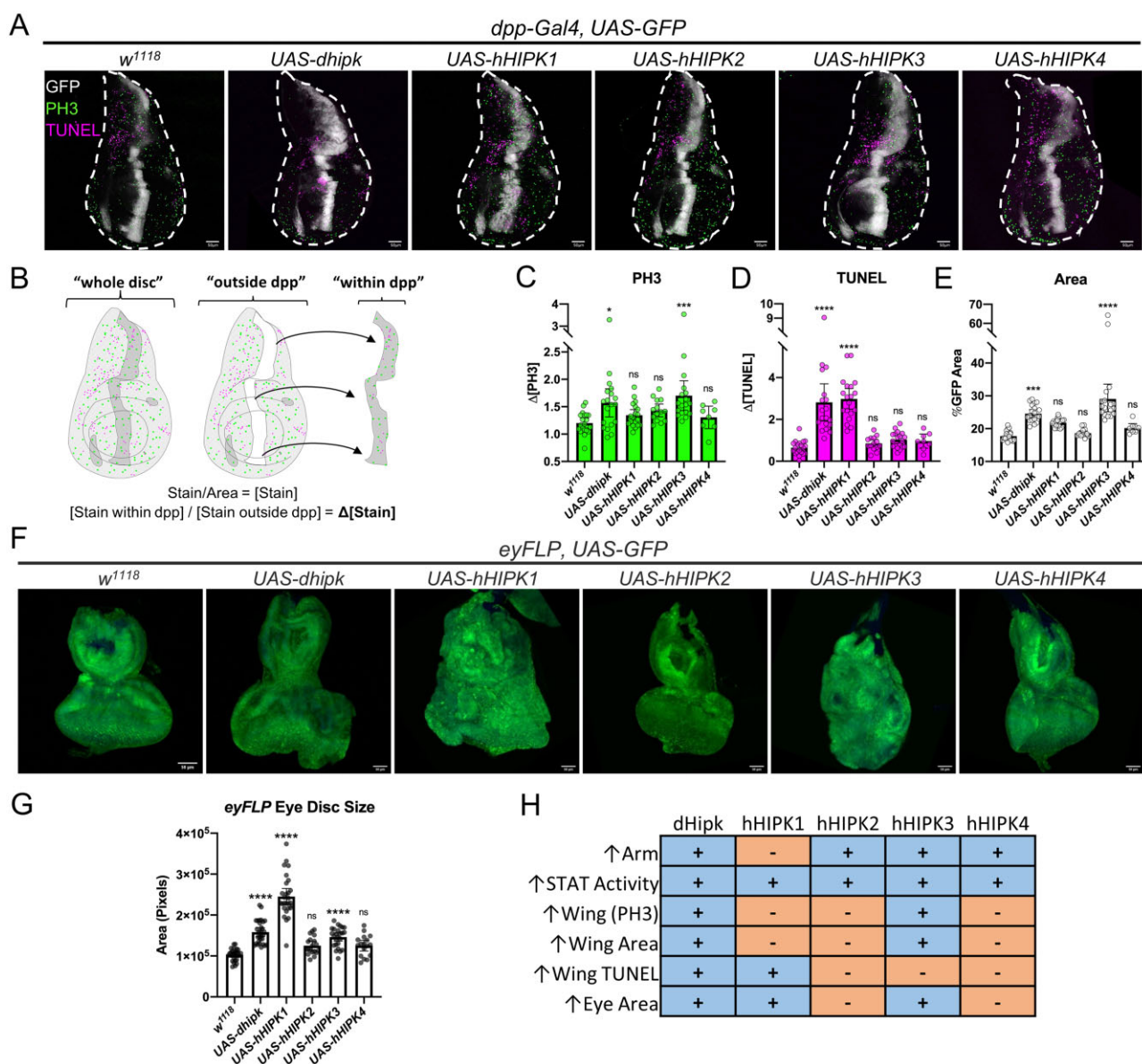


Figure 3 Human HIPKs variably induce cell proliferation, apoptosis, and tissue growth. (A) Representative images of 3rd instar imaginal wing discs of the corresponding genotypes stained for the mitotic marker PH3 (green) and the apoptosis marker TUNEL (magenta), with GFP (white) marking the *dpp-Gal4* domain where UAS constructs are expressed. Scale bars are 50 μm . (B) Diagram explaining how changes in PH3 and TUNEL stains were quantified. (C–E) Graphs show the change in PH3 staining, TUNEL staining, and area caused by expression of UAS-Hipk constructs. (F) Representative images of 3rd instar imaginal eye-antennal discs expressing UAS-Hipks and UAS-GFP using the *eyFLP* genetic construct that produces strong UAS transgene expression within the entire eye-antennal disc. (G) Graph depicting the area of eye-antennal discs measured using FIJI. For both wing and eye disc experiments, the Gal4 driver crossed to *w¹¹¹⁸* was used as the control. (H) Summary table for data presented in Figures 2 and 3. For all graphs, error bars indicate the mean with a 95% confidence interval. Statistical analysis included a one-way ANOVA followed by Dunnett's test to correct for multiple comparisons to the control sample *w¹¹¹⁸*. P-values for the statistical analyses performed correspond to the following symbols: ≥ 0.0332 (ns), < 0.0332 (*), < 0.0021 (**), < 0.0002 (***), < 0.0001 (****). Scale bars in representative images are 50 μm . Flies were raised at 29°C.

2018). Together, these data show that HIPKs variably induce proliferation, tissue growth, and apoptosis. To see if the effects of HIPKs changed when expressed in different tissues, we switched to using the *eyFLP* technique which causes high levels of Gal4 expression throughout the eye-antennal disc. In addition to dHipk and hHIPK3, hHIPK1 was also able to drastically increase tissue size, with a marked distortion of tissue morphology occurring when either hHIPK1 or hHIPK3 was expressed (Figure 3, F and G) (Pagliarini and Xu 2003). Thus, these experiments revealed that hHIPKs share many functions with dHipk, but not one single

hHIPK was able to perform all dHipk functions in these assays (Figure 3H).

hHIPK1 and hHIPK2 expression causes adult wing defects due to Ubx induction

The experiments performed above highlight the diversity of shared and unique functions of HIPKs. To further address which activities individual HIPKs can perform, we monitored adult phenotypes resulting from ectopic expression of the hHIPKs in a wildtype background. We used the *dpp-Gal4* driver, which has

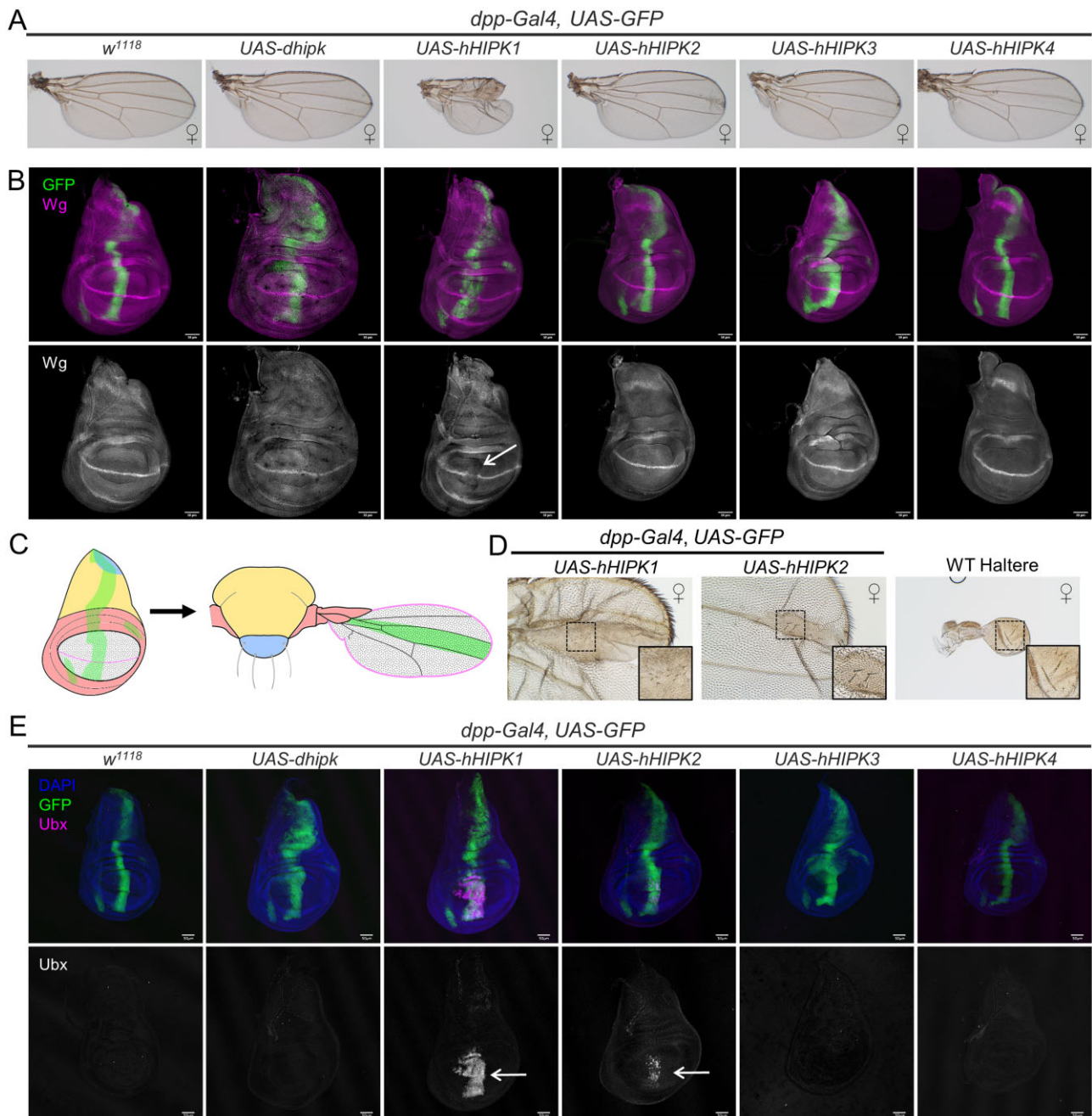


Figure 4 hHIPKs have distinct effects on wing patterning. (A) Representative adult wings dissected from the corresponding genotypes. (B) Representative images of late 3rd instar imaginal wing discs dissected from larvae of corresponding genotypes and stained for Wg. Wing discs expressing *UAS-hHIPK1* show a loss of Wg staining at the dorsal-ventral boundary (arrow). (C) Graphical representation of the *dpp-Gal4* domain in larval wing disc and adult wing tissues. Green indicates the *dpp-Gal4* domain, while other colors and patterns indicate corresponding regions between the larval and adult wing. (D) Zoomed in image of *dpp-Gal4, UAS-hHIPK1* or *UAS-hHIPK2* wing phenotype, compared to a wild-type haltere (images are to scale). Inset boxes for each image focus on similar phenotypes between the three images. (E) Representative images of late 3rd instar imaginal wing discs dissected from larvae of the corresponding genotypes and stained for the Hox protein Ubx. Wing discs expressing *UAS-hHIPK1* or *UAS-hHIPK2* show Ubx induction in the wing pouch (arrows). Results were consistent across 10 wing imaginal discs assessed for each genotype. (B,E) GFP marks the *dpp-Gal4* domain where UAS constructs are expressed. For all images, the sex of the representative tissues was picked from mixed-sex samples unless otherwise noted by the female (♀) symbol. All crosses were performed at 29°C.

well-defined and discrete expression patterns in the developing wing and leg imaginal discs (Figures 4C and 5B) (Staepling-Hampton et al. 1994). As with the pathways assessed previously in Figures 2 and 3, these experiments were carried out at 29°C to

promote obvious phenotypic changes due to high Gal4 transcriptional activity.

Expression of *UAS-hHIPK1* or *UAS-hHIPK2* caused patterning abnormalities of the adult wing when expressed using *dpp-Gal4*

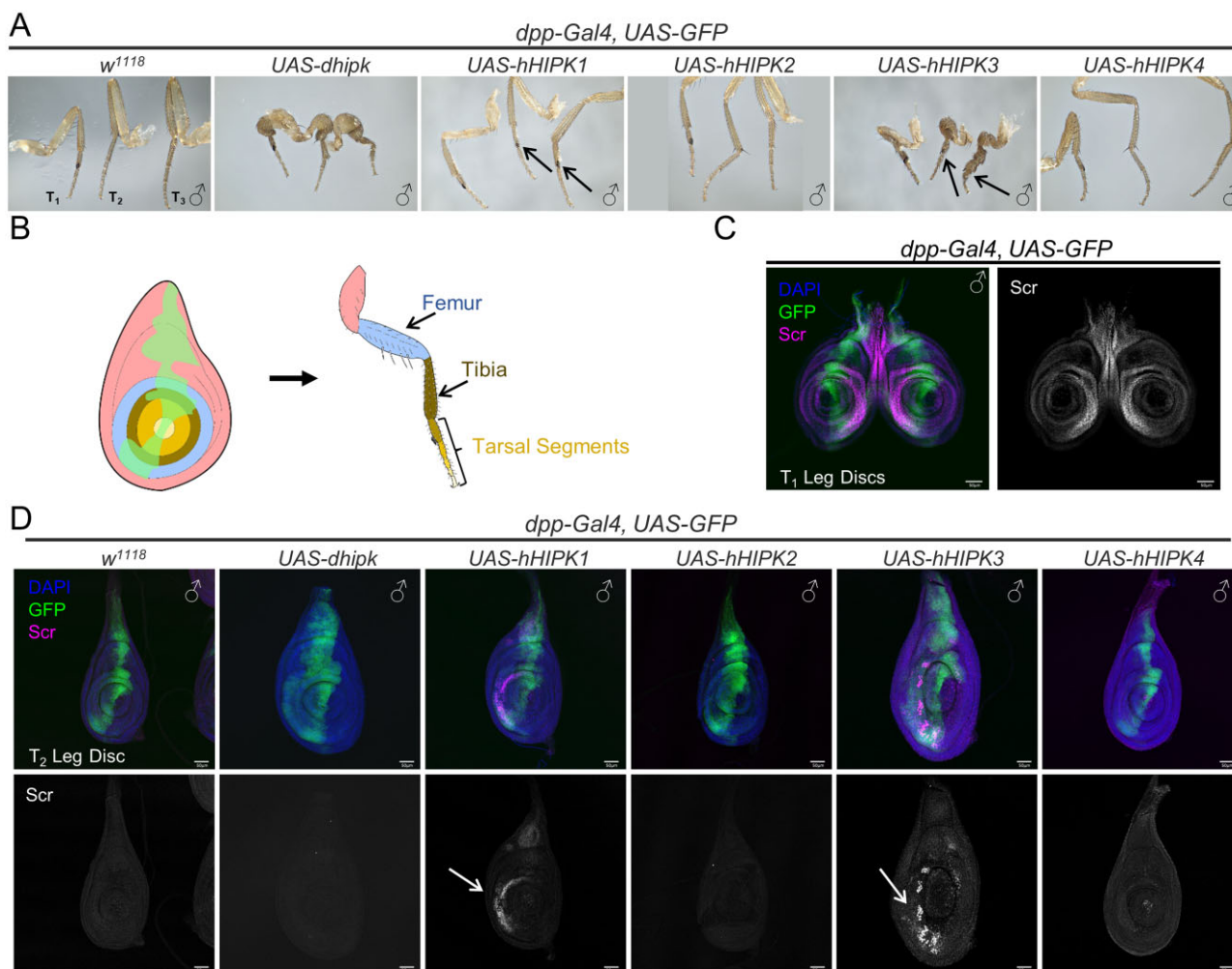


Figure 5 Leg development is differentially affected by expression of Hipks. (A) Representative adult male prothoracic (T₁), mesothoracic (T₂), and metathoracic (T₃) legs dissected from the corresponding genotypes. Arrows indicate ectopic sex combs. (B) Graphical representation of the *dpp-Gal4* domain in larval leg imaginal disc and adult leg tissues. Green indicates the *dpp-Gal4* domain, while other colors indicate corresponding regions between the larval and adult leg. (C) Image of control late 3rd instar prothoracic (T₁) imaginal leg discs stained for the Hox protein Scr. (D) Representative images of late 3rd instar mesothoracic (T₂) imaginal leg discs dissected from larvae of the corresponding genotypes and stained for the Hox protein Scr. Results were consistent across 10 T₂ imaginal leg discs assessed for each genotype. GFP marks the *dpp-Gal4* domain where UAS constructs are expressed. All adult and larval flies assessed in this figure were male. Crosses were performed at 29°C. (C,D) Scale bars: 50µm.

(Figure 4A). *UAS-hHIPK1* caused severe wing notching and vein abnormalities, while *UAS-hHIPK2* caused abnormalities to the distal central region of the wing blade, corresponding to the domain where *dpp-Gal4* is expressed (Figure 4C). Wing notching is characteristic of either disrupted Notch or Wingless signaling. Notch is required for the expression of Wingless (Wg) at the dorsal-ventral boundary, the region that specifies the edge of the adult wing blade (Rulifson and Blair 1995). The *dpp-Gal4* expression pattern in the wing disc crosses through the region that produces the adult wing margin (Figure 4C). We therefore stained 3rd instar wing imaginal discs to detect Wg while expressing each of the hHIPKs or dHipk. Wing imaginal discs expressing *UAS-hHIPK1* had reduced Wg staining where *dpp-Gal4* intersects the dorsal-ventral boundary (Figure 4B, arrow). Flies expressing *UAS-hHIPK2* show milder wing defects and appeared to have intact Wg staining, as did wing discs expressing the other Hipks.

Upon closer inspection, the region of the adult wing expressing either *UAS-hHIPK1* or *UAS-hHIPK2* contained altered wing

pigmentation, as well as small hairs and sensory bristles not normally found on the wing, instead resembling those found on the rudimentary hind wing-like structures called halteres (Figure 4D). The altered development of wing tissue causing it to fully or partially develop into haltere tissue is a homeotic transformation commonly associated with the misexpression of the homeobox (Hox) gene *Ubx* (Weatherbee et al. 1998; Pearson et al. 2005). Furthermore, *Ubx* misexpression is known to inhibit Notch's ability to regulate Wg expression at the dorsal-ventral boundary of the wing imaginal disc (Weatherbee et al. 1998). Therefore, we asked whether the phenotypes we observed could be due to ectopic *Ubx* in wing discs. We found that expression of either *UAS-hHIPK1* or *UAS-hHIPK2* caused ectopic induction of *Ubx* in the wing pouch, but not in other regions of the wing disc where *dpp-Gal4* is expressed (Figure 4E). The degree of *Ubx* induction was greater in wing discs expressing hHIPK1 compared to those expressing hHIPK2, which matches the severity of the adult wing phenotypes. Together, these data suggest that hHIPK1 and

hHIPK2 each induce ectopic *Ubx* expression in the wing pouch, resulting in a wing-to-haltere homeotic transformation.

hHIPK1 and hHIPK3 expression causes deformed legs, and *Scr*-induced ectopic sex combs

We have previously demonstrated that expression of high levels of *UAS-dHippk* in the leg using *dpp-Gal4* causes malformed adult legs due to aberrant proliferation (Figure 5A) (Wong et al. 2020). We therefore tested the effects of expressing *UAS-hHIPKs* in a discrete domain in the leg disc using *dpp-Gal4* (Figure 5B). Only *UAS-hHIPK3* caused severely malformed legs like those seen with *dHippk*, while *UAS-hHIPK1* caused less severe malformations (Figure 5A, Supplementary Table S1). In addition, we found that both *UAS-hHIPK1* and *UAS-hHIPK3* caused ectopic sex comb formation on the middle and rear legs of males, where they are not normally found (Figure 5A, arrows, Supplementary Table S1). *dpp-Gal4* is expressed in the region that gives rise to the sex combs in the leg imaginal discs (Figure 5B). The specification of sex combs requires the expression of the Hox protein Sex combs reduced (*Scr*) as seen in a control pair of the first set of leg discs called T_1 (Figure 5C). *Scr* is absent in wild-type middle legs (T_2 ; Figure 5D). We stained the T_2 leg discs with anti-*Scr* antibodies and found that those expressing *UAS-hHIPK1* or *UAS-hHIPK3* consistently showed ectopic *Scr* expression (arrows in Figure 5D). We also observed that hHIPK1 alone was able to cause loss of the antennal bristle called the arista (Supplementary Figure S3). Such an aristaless phenotype has been described as a minor antenna-to-leg transformation (Sadasivam and Huang 2016). While the Hox protein Antennapedia (*Antp*) is frequently found to be ectopically expressed in eye-antennal imaginal discs that undergo antenna-to-leg transformations, we did not observe this (data not shown) (Struhl 1981). However, partial antenna-to-leg transformations such as what we observed can occur without detectable levels of *Antp*, suggesting that *Antp* may be below the level of detection in our assay (Sadasivam and Huang 2016). Thus, hHIPKs are capable of driving ectopic expression of at least two Hox genes, *Ubx* and *Scr*, in discrete domains in specific discs.

Mutations in components of the Polycomb group complexes (PcGs), which impart epigenetic gene regulation during development, are known to result in misexpression of Hox genes in larval imaginal discs (Kassis et al. 2017). The Hox genes that are misexpressed in PcG mutants are often specific to different tissues, with *Ubx* mis-expressed in the wing imaginal disc, and *Scr* in the leg imaginal discs, similar to what we have observed with hHIPK expression using the *dpp-Gal4* driver. There is evidence for individual mutants of PcG component genes to produce different severity of Hox misexpression that depends on which component is mutated, with differences in the intensity and tissue region of ectopic Hox induction. One example provided by Beuchle et al., 2001, demonstrated the variable induction of *Ubx* and *Abdominal-B* (*Abd-B*) concomitant with individual PcG mutants in the wing imaginal disc (Beuchle et al. 2001). We therefore stained larval tissues expressing *UAS-hHIPKs* to detect *AbdB* and found that *UAS-hHIPK1* alone was able to induce ectopic *AbdB* expression in wing, leg, and eye-antennal imaginal discs (Supplementary Figure S4, A–C). Of note, the tissue regions where *AbdB* was induced in wing or leg imaginal discs were different compared to the domains where *Ubx* or *Scr*, respectively, were induced by hHIPK1.

Discussion

Vertebrate Hipks are necessary for normal development, however much remains to be learned about their individual functions. Our

incomplete understanding of the four vertebrate Hipks is exacerbated by functional redundancy, which has made it difficult to adequately study their comparative roles with individual knockouts. While cell culture studies have contributed to our understanding of Hipk functions, no work has been done to compare the ability of the four vertebrate Hipks to modulate developmental pathways in vivo. Unlike vertebrates, *Drosophila* has only a single *dHippk* that can perform many of the same functions described for vertebrate Hipks. The fly *dhipk* can also be easily knocked out, with ectopic expression of transgenic vertebrate Hipks in its place. We therefore used the fly to compare the functions of the four human HIPKs. Our results provide three key comparisons and insights. First, our rescue experiments demonstrated the extent to which each of the human HIPKs can functionally replace *Drosophila* Hipk for survival and morphological development. Second, we demonstrated the ability of each human HIPK to modulate Arm levels, JAK/STAT activity, proliferation, growth, and death, each of which have previously been described for Hipks, but never all together in comparable tissues. Third, we characterized novel phenotypes induced by human HIPKs to gain insight to their unique functions. Together, these experiments provide a direct comparison of all four vertebrate HIPKs to determine if they are capable of performing the same roles in a developmental model.

Our rescue experiments were designed to test the ability of human Hipks to rescue or suppress the pupal lethality found in *dhipk* mutant flies. Expression of hHIPKs using *Gal4* inserted in the *hipk* locus revealed that hHIPK1 and hHIPK2 each rescue *dhipk* mutant lethality, while hHIPK3 and hHIPK4 cannot. The ability of these human HIPKs to rescue *dhipk* mutants shows that they possess conserved functions. This is consistent with work from Isono et al. (2006), where *Hipk1* and *Hipk2* were shown to have overlapping roles during mouse development by analysis of double *Hipk1/Hipk2* knockouts (Isono et al. 2006). However, their work did not assess the possibility of functional redundancy between *Hipk3* or *Hipk4*. The inability of hHIPK3 or hHIPK4 to rescue *dhipk* mutant lethality in our work suggests that their roles are more divergent from those of hHIPK1 and hHIPK2, or that they are regulated differently. This is not surprising for hHIPK4, since it lacks nearly all similarities to hHIPK1, hHIPK2, and *dHippk* outside of the kinase domain (Figure 1A), however hHIPK3 is highly similar to these Hipks, so its inability to rescue *dhipk* mutant lethality may warrant further investigation into the significance of the amino acid sequence differences between these proteins.

The rescue of *dhipk* mutant lethality by hHIPK1 and hHIPK2, but not hHIPK3 or hHIPK4, provides new information in our understanding of comparative Hipk functions, however it does not tell the whole story. hHIPK2 not only rescued lethality, but also each of the head defects caused by *dhipk* knockout, which shows that it can perform multiple similar functions to *dHippk*. In comparison to hHIPK2, the ability of hHIPK1 to rescue lethality, but not any of the head defects suggests that the functions controlling lethality in the fly are distinct from those that regulate eye, ocellar, and bristle development. The idea of separate functions is further highlighted by the inability of hHIPK3 and hHIPK4 to rescue lethality while still rescuing ocellar and bristle loss, respectively, demonstrating that the four hHIPKs have varying abilities to perform *dHippk* functions. It is not clear to us how hHIPK2 was better at rescuing the *dhipk* mutant than *dHippk* itself was. We speculate that the deleterious effects of *dHippk* overexpression need to be balanced with the restoration of essential functions, and that this delicate balance is hard to achieve. However, the fact that the HIPKs are all able to affect JAK/STAT signaling to

varying degrees indicates that each of the hHIPKs are functioning adequately in the fly.

In our work, we examined the abilities of human Hipks to carry out functions that have been established for dHipk. In these studies, we expressed hHIPKS in a wildtype genetic background, and assayed a number of readouts of dHipk activity. Among these, we examined the modulation of Wnt/Wingless and JAK/STAT signaling, as well as cell proliferation, tissue growth, and apoptosis which are controlled by multiple signaling pathways, many of which are modulated by Hipks (Link et al. 2007; Lee et al. 2009b; Swarup and Verheyen 2011; Poon et al. 2012; Blaquiére et al. 2018; Tettweiler et al. 2019). Our findings revealed that human Hipks have distinct roles that are consistent with the vertebrate literature, and that none behaves exactly like dHipk, which is not unexpected. The roles of vertebrate Hipks in cell proliferation and tissue growth are conflicting and very context dependent (Blaquiére and Verheyen 2017). We found that dHipk and hHIPK3 increase proliferation and tissue growth in wing imaginal discs, while dHipk, hHIPK1, and hHIPK3 increase tissue growth in eye-antennal discs, suggesting distinct functions in different tissues. We previously found that high level expression of dHipk could induce both proliferation and apoptosis (Blaquiére et al. 2018) and in this work, we found dHipk and hHIPK1 expression led to increased apoptosis. Of note, hHIPK2, HIPK3, and HIPK4 did not increase apoptosis. These findings were notable given the well-established role for HIPK2 in promoting apoptosis. However, HIPK2 has only been described to promote p53-mediated apoptosis in conditions of cellular or genotoxic stress (D'Orazi et al. 2002; Hofmann et al. 2002). To date, the roles of HIPK3 and HIPK4 in stress-induced death are not well understood. Our experiments were not designed to promote such stresses, which may explain the absence of apoptosis when hHIPKs 2, 3, and 4 were expressed. In contrast, the ability of dHipk and hHIPK1 to induce apoptosis in the absence of cellular or genotoxic stress suggests that they use a distinct mechanism.

The ability of each of the human HIPKs to increase JAK/STAT signaling, as revealed by a STAT-responsive reporter, shows that this Hipk function is conserved across homologs, and it also indicates that this function is at least partially performed in the cytoplasm, since hHIPK4 is only found in the cytoplasm, while the other HIPKs can shuttle between the nucleus and cytoplasm (Moller et al. 2003; Arai et al. 2007; Van der Laden et al. 2015). HIPK2 was previously shown to be able to phosphorylate STAT3, which suggests other hHIPKs may also play such roles in vertebrates (Matsuo et al. 2001).

The ability of hHIPK2, hHIPK3, and hHIPK4 to increase Arm levels in the wing disc is likely due to previously described cytoplasmic activity of HIPKs, where dHipk and Hipk2 were shown to inhibit the ubiquitin ligase that targets Arm/ β -Catenin for degradation (Swarup and Verheyen 2011). HIPK1 was an outlier since it did not lead to Arm stabilization. This is most likely due to the fact that Wg protein expression is suppressed by hHIPK1, and Wg is required for Arm stabilization in signal receiving cells. One explanation for reduced Wg was the finding that hHIPK1 could induce high levels of ectopic Ubx protein. Ubx inhibits Notch signaling, thereby preventing expression of the Notch target *wingless* (Weatherbee et al. 1998). We also found that hHIPK2 causes a mild upregulation of Ubx, which could lead to reductions in Wg that were not detectable at this level of resolution, but which were apparent from the lower level of Arm stabilization, compared to the effects of hHIPK3 or hHIPK4.

In the overexpression experiments, we made a novel set of observations that expression of hHIPK1-3 could lead to homeotic

transformations, or homeosis. In each case, we found the ectopic expression of a particular Hox protein in strict tissue domains, which suggests a highly regulated process. For example, Ubx was induced only in the wing pouch region of the wing disc (Figure 4E), even though hHIPK1 was expressed in a broader domain in that disc, and no Ubx was observed in leg or eye imaginal discs, despite hHIPK1 expression in those tissues.

Hipk proteins were named for their initial discovery as binding partners of proteins containing homeodomains which are generally involved in transcriptional regulation. While several studies have found direct protein-protein interactions between Hipks and homeodomain-containing proteins such as Eyeless/Pax6 and NK3 (Kim et al. 1998, 2006; Choi et al. 1999; Steinmetz et al. 2018), it is important to note that the homeotic transformation phenotypes we observed following hHIPK expression are not indicative of direct interaction with Hox proteins. Instead, the homeotic transformations observed in these experiments are well-characterized phenotypes associated with the upregulation of Hox gene transcription (Kassis et al. 2017). Thus, Hipks appear to play dual roles with Hox proteins, in regulating their transcription (albeit indirectly, see below) and through protein-protein interactions regulating their activity.

Homeotic transformations are well-studied phenomena found to occur due to mutations in Hox genes or dysregulation of chromatin regulating complexes. Trithorax group (TrxG) and Polycomb group (PcG) complexes are two opposing types of chromatin-modifiers that epigenetically regulate Hox gene expression (Lau and So 2015). TrxG proteins promote target gene expression, while PcG proteins repress transcription through differential histone methylation. The ability of HIPKs 1, 2, and 3 to induce ectopic Hox gene expression, causing homeotic transformations, is very similar to what happens when PcG function is disrupted, or TrxG activity is enhanced (Sadasivam and Huang 2016; Kassis et al. 2017). It is therefore tempting to speculate that hHIPKs function to either promote the activity of the TrxG complex or repress the activity of PcG complexes. There is support for this model, since HIPK2 can associate with the Polycomb protein Pc2/CBX4, which is part of the Polycomb repressive complex 1 (PRC1) (Rosci et al. 2006). Another recent study used HIPK2 tethered to chromatin to directly address its ability to modulate chromosome compaction, where chromatin bound HIPK2 led to decreased Histone 3 Lysine 27 trimethylation (H3K27me3), an epigenetic mark normally associated with transcriptional repression and formation of heterochromatin (Haas et al. 2020). Thus, our findings of phenotypes associated with dysfunction of TrxG/PcG and previous work suggest that Hipks may play roles in regulating chromatin condensation. While we are not sure how the individual HIPKs induce different homeotic transformations and ectopic Hox expression, this will be an interesting area of future study, since PcG regulators are extremely important in development, and valuable to understand mechanistically in cancer (Sauvageau and Sauvageau 2010).

This study collectively shows that Hipks share many conserved functions across species and validates the use of *Drosophila* as a tool to understand this complex and multifaceted kinase family. Furthermore, our findings reveal intriguing potential roles for hHIPKs in chromatin dynamics.

Data availability

Fly strains and reagents are available upon request.

Supplementary material is available at G3 online.

Acknowledgments

The authors thank the following undergraduate students who participated in this research while training in the lab: Madeline Malczewska, Emerson Mohr, and Rayna Brands. Stocks obtained from the Bloomington Drosophila Stock Center (NIH P40OD018537) were used in this study. The *eyFLP* stock was a gift from Amit Singh. They would like to acknowledge the Developmental Studies Hybridoma Bank for providing antibodies. We thank Drs. Lienhard Schmitz and Seong-Tae Kim for donating plasmids containing *hHIPK* cDNAs. They are grateful for the advice provided by Drs. Gritta Tettweiler and Don Sinclair on various aspects of this research. Also, they thank Z. Ding for help in generating the *UAS-HA-dHipk^{attp40}* plasmid.

Funding

This work was supported by funding from the Canadian Institutes for Health Research Project Grant (E-PJT-156204) and a Natural Sciences and Engineering Research Council of Canada (NSERC) Discovery Grant (RGPIN/2014-05479).

Conflicts of interest

The authors declare that there is no conflict of interest.

Literature cited

- Arai S, Matsushita A, Du K, Yagi K, Okazaki Y, et al. 2007. Novel homeodomain-interacting protein kinase family member, HIPK4, phosphorylates human p53 at serine 9. *FEBS Lett.* 581:5649–5657.
- Bach EA, Ekas LA, Ayala-Camargo A, Flaherty MS, Lee H, et al. 2007. GFP reporters detect the activation of the Drosophila JAK/STAT pathway *in vivo*. *Gene Expr Patterns.* 7:323–331.
- Baldrige D, Wangler MF, Bowman AN, Yamamoto S, Schedl T, et al. 2021. Model organisms contribute to diagnosis and discovery in the undiagnosed diseases network: current state and a future vision. *Orphanet J Rare Dis.* 16:1–17.
- Bellen HJ, Levis RW, He Y, Carlson JW, Evans-Holm M, et al. 2011. The Drosophila gene disruption project: progress using transposons with distinctive site specificities. *188:Genetics.* 731–743.
- Bellen HJ, Levis RW, Liao G, He Y, Carlson JW, et al. 2004. The BDGP gene disruption project: single transposon insertions associated with 40% of Drosophila genes. *Genetics.* 167:761–781.
- Beuchle D, Struhl G, Müller J. 2001. Polycomb group proteins and heritable silencing of Drosophila Hox genes. *Development.* 128:993–1004.
- Blaquiere JA, Lee W, Verheyen EM. 2014. Hipk promotes photoreceptor differentiation through the repression of Twin of eyeless and Eyeless expression. *Dev Biol.* 390:14–25.
- Blaquiere JA, Verheyen EM. 2017. Homeodomain-Interacting Protein Kinases: Diverse and Complex Roles in Development and Disease. *Curr Top Dev Biol.* 123:73–103.
- Blaquiere JA, Wong KKL, Kinsey SD, Wu J, Verheyen EM. 2018. Homeodomain-interacting protein kinase promotes tumorigenesis and metastatic cell behavior. *Dis Model Mech.* 11:dmm031146.
- Chalazonitis A, Tang A. A, Shang Y, Pham TD, Hsieh I, et al. 2011. Homeodomain interacting protein kinase 2 regulates postnatal development of enteric dopaminergic neurons and glia via BMP signaling. *J Neurosci.* 31:13746–13757.
- Chen J, Verheyen EM. 2012. Homeodomain-interacting protein kinase regulates Yorkie activity to promote tissue growth. *Curr Biol.* 22:1582–1586.
- Choi CY, Kim YH, Kwon HJ, Kim Y. 1999. The homeodomain protein NK-3 recruits Groucho and a histone deacetylase complex to repress transcription. *J Biol Chem.* 274:33194–33197.
- Crapster JA, Rack PG, Hellmann ZJ, Le AD, Adams CM, et al. 2020. HIPK4 is essential for murine spermiogenesis. *Elife.* 9:e50209.
- D'Orazi G, Cecchinelli B, Bruno T, Manni I, Higashimoto Y, et al. 2002. Homeodomain-interacting protein kinase-2 phosphorylates p53 at Ser 46 and mediates apoptosis. *Nat Cell Biol.* 4:11–19.
- Duffy JB. 2002. GAL4 system in Drosophila: a fly geneticist's Swiss army knife. *Genesis.* 34:1–15.
- Gavrieli Y, Sherman Y, Ben-Sasson SA. 1992. Identification of programmed cell death *in situ* via specific labeling of nuclear DNA fragmentation. *J Cell Biol.* 119:493–501.
- Haas J, Bloesel D, Bacher S, Kracht M, Schmitz ML. 2020. Chromatin targeting of HIPK2 leads to acetylation-dependent chromatin decondensation. *Front Cell Dev Biol.* 8:852.
- Hikasa H, Sokol SY. 2011. Phosphorylation of TCF proteins by homeodomain-interacting protein kinase 2. *J Biol Chem.* 286:12093–12100.
- Hofmann TG, Jaffray E, Stollberg N, Hay RT, Will H. 2005. Regulation of homeodomain-interacting protein kinase 2 (HIPK2) effector function through dynamic small ubiquitin-related modifier-1 (SUMO-1) modification. *J Biol Chem.* 280:29224–29232.
- Hofmann TG, Möller A, Sirma H, Zentgraf H, Taya Y, et al. 2002. Regulation of p53 activity by its interaction with homeodomain-interacting protein kinase-2. *Nat Cell Biol.* 4:1–10.
- Hofmann TG, Stollberg N, Schmitz ML, Will H. 2003. HIPK2 regulates transforming growth factor-beta-induced c-Jun NH(2)-terminal kinase activation and apoptosis in human hepatoma cells. *Cancer Res.* 63:8271–8277.
- Huang H, Du G, Chen H, Liang X, Li C, et al. 2011. Drosophila Smt3 negatively regulates JNK signaling through sequestering Hipk in the nucleus. *Development.* 138:2477–2485.
- Inoue T, Kagawa T, Inoue-Mochita M, Isono K, Ohtsu N, et al. 2010. Involvement of the Hipk family in regulation of eyeball size, lens formation and retinal morphogenesis. *FEBS Lett.* 584:3233–3238.
- Isono K, Nemoto K, Li Y, Takada Y, Suzuki R, et al. 2006. Overlapping roles for homeodomain-interacting protein kinases hipk1 and hipk2 in the mediation of cell growth in response to morphogenetic and genotoxic signals. *Mol Cell Biol.* 26:2758–2771.
- Kassis JA, Kennison JA, Tamkun JW. 2017. Polycomb and Trithorax group genes in Drosophila. *Genetics.* 206:1699–1725.
- Kim YH, Choi CY, Lee SJ, Conti MA, Kim Y. 1998. Homeodomain-interacting protein kinases, a novel family of co-repressors for homeodomain transcription factors. *J Biol Chem.* 273:25875–25879.
- Kim EA, Noh YT, Ryu M-J, Kim H-T, Lee S-E, et al. 2006. Phosphorylation and transactivation of Pax6 by homeodomain-interacting protein kinase 2. *J Biol Chem.* 281:7489–7497.
- Kondo S, Lu Y, Debbas M, Lin AW, Sarosi I, et al. 2003. Characterization of cells and gene-targeted mice deficient for the p53-binding kinase homeodomain-interacting protein kinase 1 (HIPK1). *Proc Natl Acad Sci USA.* 100:5431–5436.
- Van der Laden J, Soppa U, Becker W. 2015. Effect of tyrosine autophosphorylation on catalytic activity and subcellular localisation of homeodomain-interacting protein kinases (HIPK). *Cell Commun Signal.* 13:3.[Epub].
- Lan H-C, Li H-J, Lin G, Lai P-Y, Chung B. 2007. Cyclic AMP stimulates SF-1-dependent CYP11A1 expression through homeodomain-interacting protein kinase 3-mediated Jun N-terminal kinase and c-Jun phosphorylation. *Mol Cell Biol.* 27:2027–2036.

- Lau PNI, So CWE. 2015. Polycomb and Trithorax Factors in Transcriptional and Epigenetic Regulation. In: S. Huang, M.D. Litt, C.A. Blakey, editors. *Epigenetic Gene Expression and Regulation*. Cambridge, Massachusetts: Academic Press, pp. 63–94.
- Lee W, Andrews BC, Faust M, Walldorf U, Verheyen EM. 2009a. Hipk is an essential protein that promotes Notch signal transduction in the *Drosophila* eye by inhibition of the global co-repressor Groucho. *Dev Biol*. 325:263–272.
- Lee W, Swarup S, Chen J, Ishitani T, Verheyen EM. 2009b. Homeodomain-interacting protein kinases (Hipks) promote Wnt/Wg signaling through stabilization of beta-catenin/Arm and stimulation of target gene expression. *Development*. 136: 241–251.
- Link N, Bellen HJ. 2020. Using *Drosophila* to drive the diagnosis and understand the mechanisms of rare human diseases. *Development*. 147:dev191411.
- Link N, Chen P, Lu WJ, Pogue K, Chuong A, et al. 2007. A collective form of cell death requires homeodomain interacting protein kinase. *J Cell Biol*. 178:567–574.
- Louie SH, Yang XY, Conrad WH, Muster J, Angers S, et al. 2009. Modulation of the beta-catenin signaling pathway by the dishevelled-associated protein Hipk1. *PLoS One*. 4:e4310.
- Matsuo R, Ochiai W, Nakashima K, Taga T. 2001. A new expression cloning strategy for isolation of substrate-specific kinases by using phosphorylation site-specific antibody. *J Immunol Methods*. 247:141–151.
- McGurk L, Berson A, Bonini NM. 2015. *Drosophila* as an *in vivo* model for human neurodegenerative disease. *Genetics*. 201:377–402.
- Moller A, Sirma H, Hofmann TG, Rueffer S, Klimczak E, et al. 2003. PML is required for homeodomain-interacting protein kinase 2 (HIPK2)-mediated p53 phosphorylation and cell cycle arrest but is dispensable for the formation of HIPK domains. *Cancer Res*. 63: 4310–4314.
- Pagliarini RA, Xu T. 2003. A genetic screen in *Drosophila* for metastatic behavior. *Science*. 302:1227–1231.
- Papadopoulos JS, Agarwala R. 2007. COBALT: constraint-based alignment tool for multiple protein sequences. *Bioinformatics*. 23: 1073–1079.
- Pearson JC, Lemons D, McGinnis W. 2005. Modulating Hox gene functions during animal body patterning. *Nat Rev Genet*. 6:893–904.
- Peifer M, Sweeton D, Casey M, Wieschaus E. 1994. wingless signal and Zeste-white 3 kinase trigger opposing changes in the intracellular distribution of Armadillo. *Development*. 120:369–380.
- Poon CLC, Zhang X, Lin JI, Manning SA, Harvey KF. 2012. Homeodomain-interacting protein kinase regulates Hippo pathway-dependent tissue growth. *Curr Biol*. 22:1587–1594.
- Rinaldo C, Siepi F, Prodosmo A, Soddu S. 2008. HIPKs: jack of all trades in basic nuclear activities. *Biochim Biophys Acta*. 1783: 2124–2129.
- Rochat-Steiner V, Becker K, Micheau O, Schneider P, Burns K, et al. 2000. FIST/HIPK3: a Fas/FADD-interacting serine/threonine kinase that induces FADD phosphorylation and inhibits Fas-mediated Jun NH(2)-terminal kinase activation. *J Exp Med*. 192:1165–1174.
- Roscic A, Möller A, Calzado MA, Renner F, Wimmer VC, et al. 2006. Phosphorylation-dependent control of Pc2 SUMO E3 ligase activity by its substrate protein HIPK2. *Mol Cell*. 24:77–89.
- Rulifson EJ, Blair SS. 1995. Notch regulates wingless expression and is not required for reception of the paracrine wingless signal during wing margin neurogenesis in *Drosophila*. *Development*. 121: 2813–2824.
- Sadasivam DA, Huang D-H. 2016. Maintenance of tissue pluripotency by epigenetic factors acting at multiple levels. *PLoS Genet*. 12:e1005897.
- Sauvageau M, Sauvageau G. 2010. Polycomb group proteins: multi-faceted regulators of somatic stem cells and cancer. *Cell Stem Cell*. 7:299–313.
- Schindelin J, Arganda-Carreras I, Frise E, Kaynig V, Longair M, et al. 2012. Fiji: an open-source platform for biological-image analysis. *Nat Methods*. 9:676–682.
- Schindelin J, Rueden CT, Hiner MC, Eliceiri KW. 2015. The imageJ ecosystem: an open platform for biomedical image analysis. *Mol Reprod Dev*. 82:518–529.
- Schneider CA, Rasband WS, Eliceiri KW. 2012. NIH Image to ImageJ: 25 years of image analysis. *Nat Methods*. 9:671–675.
- Shimizu N, Ishitani S, Sato A, Shibuya H, Ishitani T. 2014. Hipk2 and PP1c cooperate to maintain Dvl protein levels required for Wnt signal transduction. *Cell Rep*. 8:1391–1404.
- Shojima N, Hara K, Fujita H, Horikoshi M, Takahashi N, et al. 2012. Depletion of homeodomain-interacting protein kinase 3 impairs insulin secretion and glucose tolerance in mice. *Diabetologia*. 55: 3318–3330.
- Sjölund J, Pelorosso FG, Quigley DA, DelRosario R, Balmain A. 2014. Identification of Hipk2 as an essential regulator of white fat development. *Proc Natl Acad Sci USA*. 111:7373–7378.
- Staebling-Hampton K, Jackson PD, Clark MJ, Brand AH, Hoffmann FM. 1994. Specificity of bone morphogenetic protein-related factors: cell fate and gene expression changes in *Drosophila* embryos induced by decapentaplegic but not 60A. *Cell Growth Differ*. 5:585–593.
- Steinmetz EL, Dewald DN, Walldorf U. 2018. Homeodomain-interacting protein kinase phosphorylates the *Drosophila* Paired box protein 6 (Pax6) homologues Twin of eyeless and Eyeless. *Insect Mol Biol*. 27:198–211.
- Struhl G. 1981. A homoeotic mutation transforming leg to antenna in *Drosophila*. *Nature*. 292:635–638.
- Swarup S, Verheyen EM. 2011. *Drosophila* homeodomain-interacting protein kinase inhibits the Skp1-Cul1-F-box E3 ligase complex to dually promote Wingless and Hedgehog signaling. *Proc Natl Acad Sci USA*. 108:9887–9892.
- Tettweiler G, Blaquiére JA, Wray NB, Verheyen EM. 2019. Hipk is required for JAK/STAT activity during development and tumorigenesis. *PLoS One*. 14:e0226856.
- Ugur B, Chen K, Bellen HJ. 2016. *Drosophila* tools and assays for the study of human diseases. *Dis Model Mech*. 9:235–244.
- Uhlén M, Fagerberg L, Hallström BM, Lindskog C, Oksvold P, et al. 2015. Tissue-based map of the human proteome. *Science*. 347: 1260419.
- Waterhouse AM, Procter JB, Martin DMA, Clamp M, Barton GJ. 2009. Jalview Version 2—a multiple sequence alignment editor and analysis workbench. *Bioinformatics*. 25:1189–1191.
- Weatherbee SD, Halder G, Kim J, Hudson A, Carroll S. 1998. Ultrathorax regulates genes at several levels of the wing-patterning hierarchy to shape the development of the *Drosophila* haltere. *Genes Dev*. 12:1474–1482.
- Wong KKL, Liao JZ, Verheyen EM. 2019. A positive feedback loop between Myc and aerobic glycolysis sustains tumor growth in a *Drosophila* tumor model. *Elife*. 8:e46315.
- Wong KKL, Liu TW, Parker JM, Sinclair DAR, Chen YY, et al. 2020. The nutrient sensor OGT regulates Hipk stability and tumorigenic-like activities in *Drosophila*. *Proc Natl Acad Sci USA*. 117:2004–2013.